Z. Phys. Chem. **223** (2009) 169–181 / **DOI** 10.1524/zpch.2009.6031

Size and Structure of Palladium Clusters Determined by XRD and HREM

By M. Suleiman[1,*], C. Borchers[1], M. Guerdane[1], N. M. Jisrawi[2], D. Fritsch[3], R. Kirchheim[1], and A. Pundt[1]

[1] Institute of Material Physics, University of Göttingen, 37077 Göttingen, Germany
[2] Physics Division, College of Arts and Sciences, University of Sharjah, POB 27272, Sharjah, UAE
[3] GKSS Research Centr Geesthacht GmbH, Institute of Polymer Research, 21502 Geesthacht, Germany

Dedicated to Prof. Dr. Klaus Christmann on the occasion of his 65th birthday

(Received October 8, 2008; accepted October 17, 2008)

Palladium / Cluster / XRD / HREM

Scherrer formula is often applied to X-ray-diffraction profiles for the size determination of small size clusters. However, for small clusters this often leads to conflicting results in comparison to other methods. A series of Pd-clusters of different size is studied by X-ray diffraction analysis and transmission electron microscopy. The influence of size and structure on the results is presented and discussed in comparison with theoretical calculations. It will be shown that the different structure of small size systems are one main origin of the conflicts. The structure problem can be overcome by using Fourier Transform of the X-ray diffraction pattern. The importance of the knowledge of the cluster structure was demonstrated by showing its strong influence on the hydrogen solubility.

1. Introduction

Nanoparticles named "clusters" are agglomerates of a few hundred to a few thousand atoms with total radii less than 50 nm. Recently there is intense scientific interest in nanoparticles. The chemical and physical properties of such aggregates are in a transition region between the bulk and the individual atomic or molecular properties [1].

A particularly interesting application is the possibility of using arrays of nanoparticles for fabrication of single electron tunnelling devices [1]. Catalysis

* Corresponding author. E-mail: suleiman@ump.gwdg.de

is another field in which nanosciences have been applied for many years [2, 3]. The aim of having a catalyst with maximum active area exposed to a chemical reaction has produced enormous amount of research in nanoparticles. Particularly, transition metal nanoparticles are a very important field in catalysis. Recently, H-storage in nano-particles has become a field of interest. Here, the fast kinetics due to short diffusion lengths is a major advantage, but, also, there is a hope on advantageous storage properties of the nano-system.

Attractive methods to characterise the structure and size of nanometer transition particles are X-ray analysis, transmission electron microscopy (TEM) and high resolution transition electron microscopy (HRTEM). Debye-Scherrer diffraction patterns are often used to characterise samples, as well as to probe the structure of nanoparticles. In practice, problems with interpretation of an X-ray diffraction pattern begin when the lattice parameters obtained from two peaks, corrected for errors, differ by more than 0.01 Å and the intensities of the peaks quickly approach background levels at high scattering angles. Then, one departs the region where the Scherrer formula [4, 5] is accurate in estimating the nanoparticles size. This formula is derived assuming that the diffraction peak is associated with a family of crystal planes is a size-limited crystal. The existence of the so-called multiply twinned particles (MTP) or even the high proportion of atoms at the surface of aggregates means that translational symmetry is not an underlying feature of nanoparticles. To associate diffraction features with the notion of Bragg peaks from a family of crystal planes is unwise in this case. Diffraction patterns are better thought of as a superposition of continuous oscillatory function in reciprocal space [6].

At present, modern electron microscopy can give resolution of less than 0.2 nm, which is sufficient to characterise cluster cores of the heavier transition metals at atomic resolution. However, HRTEM analyses do have a disadvantage, since the energy of the electron beam can be as much as 400 keV, the particles under investigation are heated up rapidly and rearrangement and coalescence process may result. This is especially true for smaller clusters (1–4 nm) where the melting point is largely reduced and is a function of the particle size [7]. To maintain the cluster size during the experiment and to exclude cluster coalescence, stabilizers are needed. Often, surfactants are used that stabilize clusters by sterical exclusion.

In this work we compare common TEM, HRTEM and XRD methods for structure and size evaluation with respect to the model system of Pd-clusters. The focus will be on problems occurring when the cluster structure changes. For clarity this will be done with respect to model cluster calculations. Additionally, we will demonstrate the influence of the cluster structure on the hydrogen solubility.

2. Experimental

2.1 Samples preparation and characterization

Pd clusters are synthesised by an electrochemical method [8], in which a simple electrolysis cell consisting of two electrodes (a Pd anode and cathode) is used. The electrolyte contains the stabilizer (surfactant) in solved form. Here, Tetraoctylammonium bromide (TAOB) is used. Applying constant current to the electrodes causes dissolution of the anode material, which reduced in the vicinity of the cathode into the so called ad-atoms. In the electrolyte the ad-atoms aggregate into clusters, which are stabilised by TOAB that weakly binds to the metal surface by the negative charge of the N-ion. Three octyl-arms touch the cluster while fourth sticking-out octyl-arm separates each two clusters by about 2 nm. This method has many advantages over other method such as very narrow size distribution and the quasi-free nature of the stabilised clusters [8].

X-ray diffraction measurements were performed on beam line B2 at the synchrotron laboratory HASYLAB at DESY in Hamburg. The wavelength was selected by a Ge(111) double-crystal monochromator, all samples were measured at λ = 1.120599 Å.

TEM was performed with a Philips EM 420 ST microscope (resolution limit 0.3 nm, information limit 0.2 nm, accelerating voltage 120 kV). TEM specimens were prepared by scooping them from the solution on a grid (Ø = 3 mm, 400 mesh) that is coated with a carbon film. The method of preparation included dipping the grid in the solution of TOAB-stabilised palladium clusters (about 10^{-4} M) for a few seconds. This was followed by the removal from the solution. Afterwards, the grid was dried at room temperature for several hours.

HRTEM was then performed using Philips CM200 FEG UT (FEG = field emission gun, UT ultra twin) with an accelerating voltage of 200 kV.

2.2 Cluster size estimation from a Fourier Transform

The intensity, i.e. the energy per unit cross section per unit time, scattered by an aggregate of N atoms is given by

$$I(k) = I_o \sum_{i,j=1}^{N} f_i f_j \exp[i\vec{k}(\vec{r_i} - \vec{r_j})]$$

where, I_o is the incident intensity, f_i is the atomic scattering factor for atom i, k is the scattering vector for the scattered plane wave, and r is the position of the atom i [9, 10].

For the particular case of a one-component system with an isotropic distribution in space of the interatomic vectors $\vec{r}_{ij} = \vec{r}_i - \vec{r}_j$, the averaging over all directions can be performed for a fixed length, and one obtains by introducing the radial distribution function (r.d.f) $P(r)$:

$$I(k) = I_o N f^2 + I_o N f_o \int P(r) \cdot \frac{\sin kr}{kr} \cdot dr$$

Where $k = 4\pi\sin\theta/\lambda$, f_O is the average number density of atoms in the sample and θ is half the scattering angle and λ is the wavelength of the radiation. *P(r)* is related to the experimental scattered intensity by a simple Fourier transform as we can see from

$$P(r) = r\int k\cdot[S(k)-1]\cdot\sin kr\cdot dk$$

The structure factor, *S(k)*, is related to the intensity *I(k)* via:

$$S(k) = \left[\frac{I(k)}{f^2 NI_o} - 1\right]$$

The r.d.f. is the most important quantitative information obtained from diffraction experiments. In the case of nearly spherical nanoparticle samples, the position of the last visible peak of the r.d.f. gives a fairly accurate value of the sample size. This is, however, possible only if the r.d.f. can be determined with a sufficient resolution, depending strongly on the extension of the wave vector interval [$k_{\min}$, $k_{\max}$.], over which the intensity *I(k)* has been measured. If this interval is too limited to include most diffraction details, strong oscillations affect the form of the r.d.f. making the identification of the small peaks at large distances and hence the determination of the actual sample size, impossible. Hall et al. showed, however, that even in these conditions and in spite of the strong oscillations and poor spatial resolution of the r.d.f., the attenuation of this oscillating feature is related to the nearly spherical form of the nanoparticle and can be used to give a good estimation of their average diameter.

Since I and N are unknown in the case of a nanoparticle solution, Hall et al. suggested to Fourier-transform the measured scattering intensity into real space by calculating

$$P(r) = \beta r\int_{k_{\min}}^{k_{\max}} k\cdot M(k)\left[\frac{I(k)}{\alpha f^2} - 1\right]\sin kr\cdot dk$$

α and β are parameters that must be estimated and *M(k)* a Lanczos function. Where

$$M(k) = \frac{\sin ka}{ka} \text{ and } a = \frac{\pi}{k_{\max}}.$$

The Lanczos function has been used by Hall et al. [6] in order to damp the spurious oscillations in the Fourier transform caused by the abrupt truncation at the upper limit of the diffraction data and getting more intense if the range of the measured scattering wave vector is reduced.

3. Results and discussions

3.1 Cluster size determination

In this section determination of the cluster size will be discussed using XRD and TEM results. The estimation of the cluster size using XRD data will be done by

Table 1. Comparison of the Pd cluster size [nm] for different samples obtained from XRD data by using Scherrer formula and TEM.

Sample No.	Cluster size [nm]	
	XRD	TEM
c	2.2	3.6 ± 0.4
b	3.5	5.0 ± 0.6
a	6.0	5.6 ± 1. 1

two methods: First by using the Scherrer formula, and second by taking a Fourier transform of a diffraction pattern. This will be compared with the size obtained for Pd model clusters in two different lattice structures. These model clusters were received by molecular dynamics simulations using embedded atom potentials of Daw and Baskes [11].

Table 1 summarizes the cluster sizes obtained, for the same sample prepared by electrochemical method, by Scherrer formula from XRD-pattern and from TEM image analyses. The obtained sizes differ strongly. This problem arises because of the variety of structures and the size dependent nature of the diffraction pattern [5]. Difficulties in applying the peak-width based analysis to clusters have been reported by a number of workers [5, 12]. On one hand, the small size as well as the mechanical stress in clusters leads to peak broadening [13]. Also there are indications that the outermost shells of a cluster are closer to the second most outer shell than all the other inter-shell distances [14]. On the other hand, the structure of the clusters may change thereby leading to completely new diffraction patterns. If five-fold symmetry structures arise, peak interpretation becomes difficult.

In this work we have found that estimations of the Pd cluster size from XRD data using Scherrer formula for Pd cluster samples, in most cases, give values smaller than those obtained by TEM method, as shown in Table 1. We attribute this difference in the cluster size for the same sample obtained by the two methods to an icosahedral structure of the Pd clusters. The presence of an icosahedral structure will lead to peak broadening which means that estimations of the size of an icosahedral cluster using the XRD data will give a smaller value than the real size. In the following this will be demonstrated by a model cluster.

Figure 1 shows the XRD patterns for a model Pd cluster (2057 atoms about 3.7 nm) obtained by MD-simulation from two different lattices, (a) cubic and (b) icosahedral, [15]. It is clearly visible that the diffraction pattern of the icosahedral cluster reveals broader peaks than those for the cubic one. Estimation of the cluster size for the peak width ((111) peak) using the Scherrer formula gives a size of 3.6 nm for the cubic cluster and 2.2 nm for the icosahedral cluster. As known from the input clusters, this difference is not real and it is due to peak broadening resulting from the strained icosahedral structure compared to the cubic structure.

A comparison will confirm the strength of the method proposed by Hall et al. [6], where information related to the average distribution of the interatomic

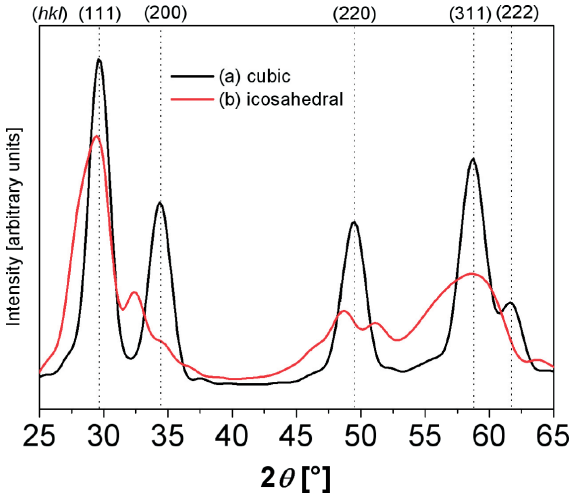

Fig. 1. Diffraction patterns of a model Pd cluster consisting of 2057 atoms: (a) shows the diffraction pattern of a cubic cluster (3.7 nm), (b) represents an icosahedral cluster (3.7 nm). The dotted vertical lines are the position of the Bragg reflections for bulk Pd with cubic lattice structure after [15].

distances within the cluster is obtained and the last visible peak of the radial distribution function (r.d.f) or P(r) gives a fairly accurate value of the sample size. Figure 2 shows the Fourier transform of the diffraction patterns of the icosahedral and cubic model clusters shown in Fig. 1. For both cluster structures there is a trend of decreasing oscillation in the P(r) with increasing interatomic distance. In both cases the oscillations vanish at an interatomic distance of 3.7 nm. This is in good accordance with the real size of both (2057 atoms) model clusters and verifies the method of Hall et al. for Pd-clusters.

Figure 3(a–c) shows the diffraction patterns of three different TOAB-Pd cluster samples. The cluster sizes obtained from the application of the Scherrer formula are: (a) 6.0 nm, (b) 3.5 nm and (c) 2.2 nm. Figure 3 (a–c) shows, also, the TEM analyses of these samples. One obtains: (a) 5.6 ± 1.1 nm, (b) 5.0 ± 0.6 nm and (c) 3.6 ± 0.4 nm. These values, again, differ from those obtained from XRD data. This difference is attributed to different cluster structures of the samples. This will be confirmed in the next section. The smaller XRD size values obtained in (b) (3.5 nm from XRD 5.0 nm from TEM) and in (c) (2.2 nm from XRD and 3.6 nm from TEM) are due to the iscoahedral structure of these cluster samples. The larger XRD value obtained for (a) is due to the cubic structure of this cluster sample and the wide size distribution where larger particles contributed more to the intensity.

Hall's method was also applied to these experimental data. The Fourier Transform of these samples is shown in Fig. 4(a–c). The estimated cluster size for each sample is marked with the grey rectangular region indicating uncertainty

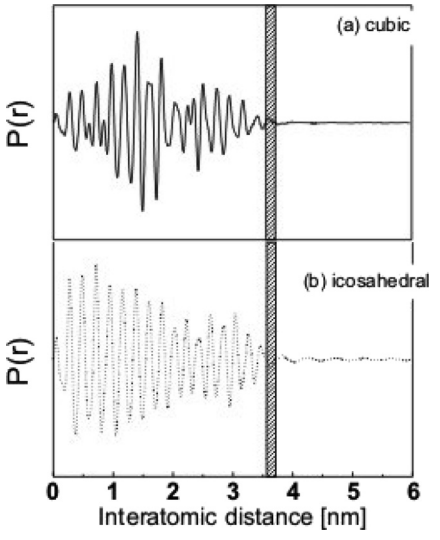

Fig. 2. P(r) for a model Pd cluster (a) cubic, (b) icosahedral. In both cases the P(r) oscillations vanish at inter atomic distance of about 3.7 nm.

intervals around the size estimates: (a) 6.5 ± 0.5 nm, (b) 5.0 ±0.5 nm and (c) 3.0 ± 0.5 nm. For simplicity, we did not implement the damping function in the data conversion. As can be seen, the obtained values are fairly similar to the results obtained by TEM image analyses. Thus, also XRD patterns can be used to gain accurate cluster sizes when Hall's method is applied. However, in the following, we will use the sizes obtained by TEM studies only.

3.2 Cluster structure

The structure of the Pd clusters was determined by two independent methods, HRTEM and XRD. Although HRTEM is one of the most useful techniques to determine the structure, it has the disadvantage of illuminating the sample with a high energy source, in our case 200 keV. In some cases it can be as high as 400 keV. This could lead to structural fluctuations of the nanometer-sized cluster and a mixture of structures could be obtained. In contrast, XRD is a possible technique which is also powerful in determining the structure. This will be shown by calculating diffraction pattern from model clusters up to 2057 atoms (about 3.7 nm), obtained by MD-simulations.

In the XRD patterns of 3.7 nm Pd model clusters of Fig. 1 (a) and (b) are important and significant differences between the two patterns. The cubic cluster, Fig. 1, line (a), has diffraction patterns similar to that of bulk Pd, both in position and intensity, as confirmed by multi-Gaussian fits. The icosahedral cluster, Fig. 1 line (b), has a much different diffraction pattern. These differences are: First, the

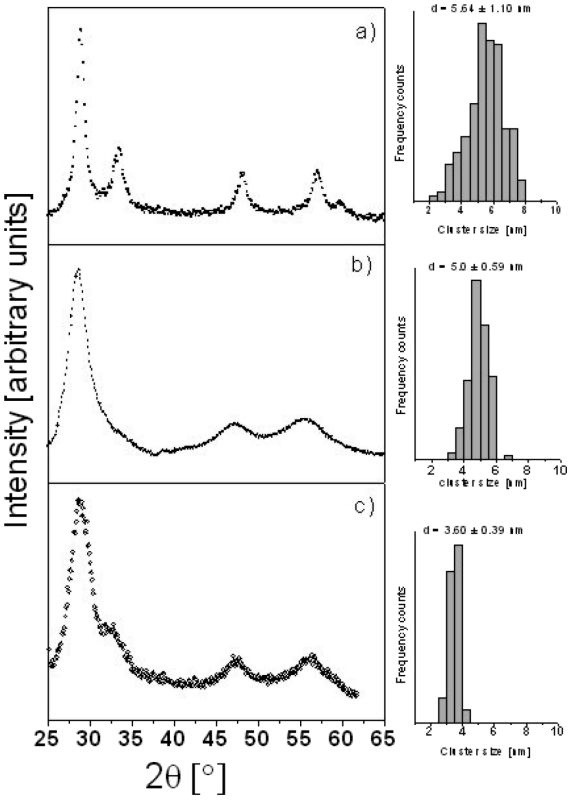

Fig. 3. Diffraction patterns of three different samples of electrochemically prepared Pd clusters: sample (a), sample (b) and sample (c). On the side of the diffractogram of each sample the size distribution of the sample obtained by TEM is shown.

integrated intensity of the second diffraction peak (near bulk (200)) has a smaller value in comparison to the integrated intensity of the first (near bulk (111)) peak. Second, the angular separation with $2\theta = 2.5$ ° between the first peak (near bulk (111)) and the second peak (near bulk (200)) is much less in comparison to that of the bulk with $2\theta = 5.0$ °. Third, an increased intensity in the diffractogram of the icosahedral cluster between 51 and 56 degrees is also observed.

In Fig. 3 (a–c), we have shown the XRD patterns of three different experimental cluster samples ((a) 5.6 nm, (b) 5.0 nm and (c) 3.6 nm (as determined by TEM)) In Fig. 3 (b) and (c), there is a considerable intensity decrease in some diffraction peaks (near bulk (200) and (222)) in comparison with that of the near bulk (111) diffraction pattern. In addition, there is an intensity increase between 51 and 56 degrees in the diffractogram of the 3.6 nm and 5.0 nm clusters which was not found for the 5.6 nm clusters, see Fig. 3(a). Furthermore, the reflection close to the bulk (200) peak position is slightly shifted towards the reflection

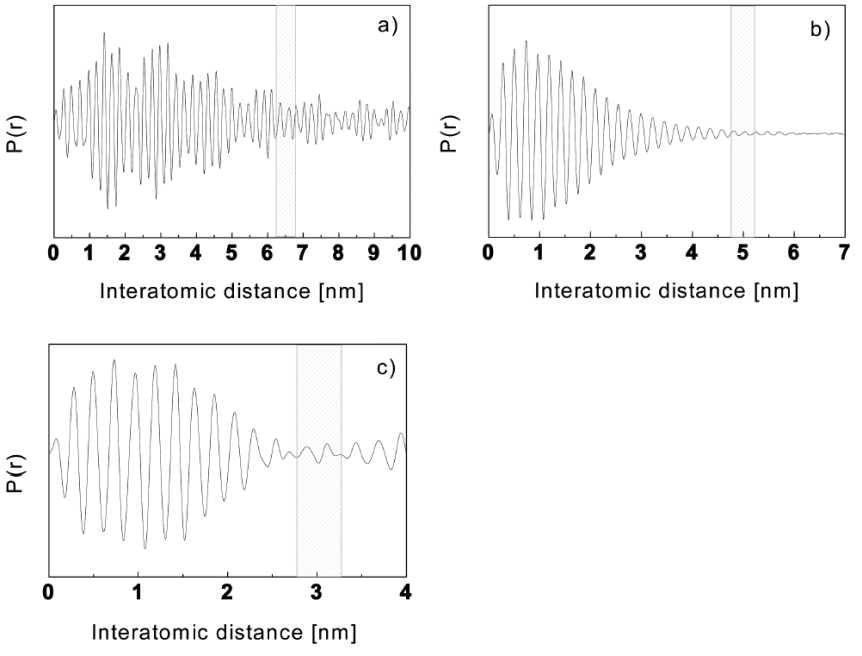

Fig. 4. Profiles (a) through (c) show the results of inverting the diffraction patterns of Fig. 3. The grey rectangular region indicates the uncertainty interval around the estimated Pd Cluster size.

near the bulk (111) peak position. Comparing the experimental XRD patterns with those obtained from MD-simulated clusters, one can see that the 5.6 nm clusters have a cubic lattice structure, while the 3.6 nm and the 5.0 nm clusters have predominantly icosahedral lattice structure. This directly explains the smaller size value obtained when estimating the cluster size of the last two samples using the Scherrer formula as we have seen in the previous section.

The structure of clusters was also determined by analysing the HRTEM images of about 50 particles. Fast Fourier transformation analysis (FFT) of the 5.6 nm clusters sample shows that most of particles (90 %) have cubic lattice structure, 5 % are icosahedral and others are multi-twinned. Figure 5 shows three HRTEM images of three single clusters of this sample and the corresponding FFT analysis. Figure 5(a) shows a cubic particle and its corresponding FFT. In the HRTEM image the (111) planes are clearly seen as columns of atoms that appear as black dots. In the corresponding FFT of this particle two dots are visible indicating that the particle is in the 111 orientation. In the HRTEM images cubic lattices easily show lattice fringes (straight lines) when rotated in the proper direction.

Figure 6 shows the HRTEM and corresponding FFT images of the 5.0 nm cluster, most of the particles (95 %) have icosahedral structure as can be seen in

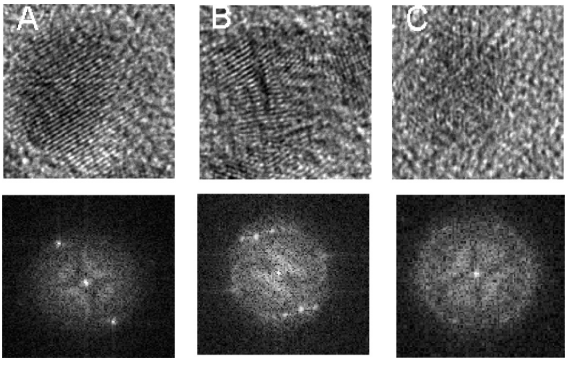

Fig. 5. HRTEM images and diffraction images of the 5.6 nm cluster: 90% of the clusters have cubic structure (A). The rest are multi-twinned (B) or icosahedral (C).

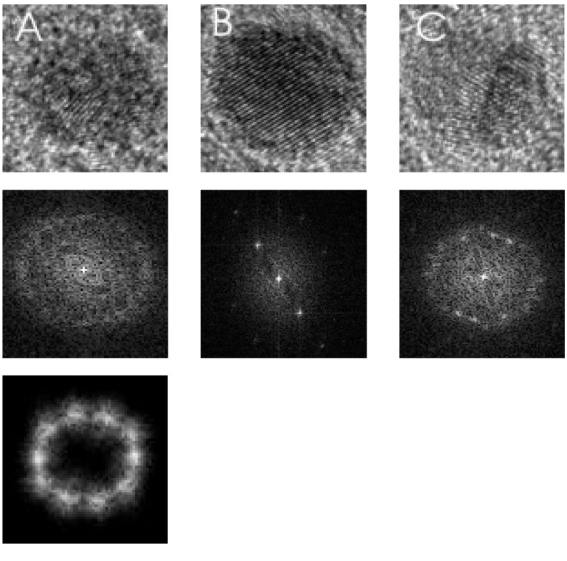

Fig. 6. HRTEM of and FFT image of the 5.0 nm Pd cluster: 95% of the particles have icosahedral structure (A), the rest is face centred cubic (B) or multi-twinned (C). (A) bottom shows the FFT images after removing the background.

Fig. 6 (a). Although there is some background noise 10 spots in the FFT can be identified, corresponding to five fold symmetry. Back-Fourier-transformation of the HRTEM diffraction pattern just containing the ten most intensive spots yields a cluster image similar to the original one. This verifies that the major information is focussed in these diffraction spots and further, that the clusters possess five-fold symmetry. Very limited number of clusters are cubic or single-twinned

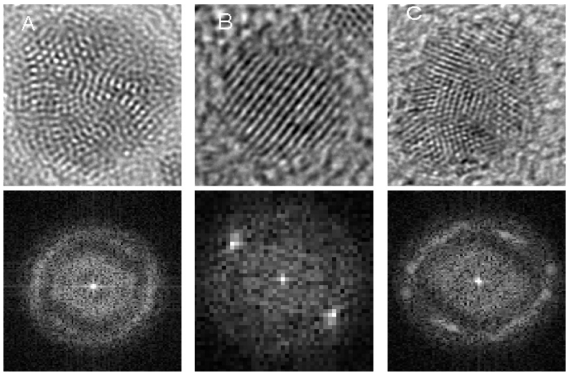

Fig. 7. HRTEM and FFT images of the 3.6 nm Pd clusters: 95% of the particles have icosahedral structure (A). The rest is cubic (B) or multi-twinned (C).

particles, as shown in Fig. 6 (b) & (c). Generally, icosahedral clusters do not lay in the desired five fold symmetry direction and it is not possible to rotate them into the five-fold symmetry direction. Then, one needs to determine the cluster structure only from the HRTEM image. In this case, no straight lattice fringes are visible but an amorphous-like pattern. In some cases, other patterns, resulting from the two-or three- fold symmetry direction are visible. However, even in these cases no straight lattice fringes but curved lines are visible.

Figure 7 shows the HREM of 3.6 nm (TEM) Pd cluster sample. FFT of HRTEM images show that most of the particles (95 %) have an icosahedral lattice structure. Exemplarily, in Fig 7(a), although there is some background noise, one can see 10 spots in the FFT corresponding to the five fold symmetry. Few particles are cubic and some are multi-twin particles (Fig. 7 (b) &(c)).

The HRTEM image analyses and diffraction pattern confirm the results obtained from XRD data analyses. To conclude, for Pd-clusters both methods can be successfully applied to gain information about cluster structure and size.

3.3 Impact of cluster structure on H-solubility

Palladium metal is known to solve hydrogen under ambient conditions. It is solved in interstitial lattice sites as well as at surface sites [16]. The content of hydrogen in the clusters can be varied by changing the hydrogen gas pressure, the higher the pressure, the larger the H-content. The hydrogen solubility of clusters with different structure but same size shows large differences, as exem-

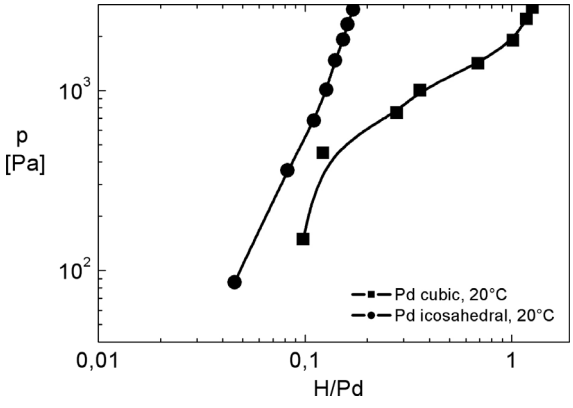

Fig. 8. Isotherms of 3.1 nm cubic and icosahedral clusters. The solubility of cubic clusters is always increased compared to icosahedral clusters.

plarily shown in Fig. 8. There, isotherms of two samples of 3.1 nm cluster diameter are summarized, indicating the strong change especially for small H-concentrations. Details about the cluster preparation are published in ref. [8, 17]. Both curves, furthermore, differ from that of the bulk system. For cubic clusters, H is first preferentially solved in surface- and subsurface sites and, at higher concentrations, also solved in inner sites [18]. The isotherm shows a plateau-like region in the pressure range where bulk samples also show a plateau. This was attributed to a phase transformation. However, icosahedral clusters show a much different isotherm with no plateau. The maximum solubility is also affected by the structure: it is much reduced for the icosahedral structure compared to the cubic one. To conclude, the cluster structure has a major impact on the hydrogen solubility and has to be considered especially when hydrogen storage is of interest.

4. Summary

Small metal clusters reveal structures that strongly differ from structures known for bulk metals. Application of the Scherrer formula on XRD-diffraction line profiles, then, results in conflicting cluster size determination compared to TEM. Using XRD diffraction pattern fourier analyses results in good agreement with TEM observations on the same clusters. It was demonstrated that conflicting results mainly result from the different structures of small particles. Furthermore, it was shown that the cluster structure has a strong influence on the hydrogen solubility.

Acknowledgement

Financial support by the DFG via project PU 131/6–1 is gratefully acknowledged. Beam time provided by HASYLAB, Hamburg, Germany is highly appreciated.

References

1. G. Schmidt (Ed.), *Cluster and colloids*. VCH Weinheim (1994).
2. R. Elghanian, J. Storhoff, R. C. Mucic, R. L. Letsinger, C. A. Mirkin, Science **277** (1997) 1078.
3. L. N. Lewis, Chem. Rev. **93** (1993) 2693.
4. Z. Kaszkur, J. Appl. Cryst. **33** (2000) 87.
5. P. Scherrer , Nachr. Göttinger Gesellsch. (1918) 98.
6. B. D. Hall, D. Zanchet, D. Ugarte, J. Appl. Cryst. **33** (2000) 1335.
7. M. Takagi, J. Phys. Soc. Jpn. **9** (1954) 359.
8. M.T. Reetz, W. Helberg: J. Am. Chem. Soc. **116** (1994) 7401.
9. P. Debye, Ann. Physik **46** (1915) 809.
10. A. Guinier, *Théorie de la cristallographie*. Dunod, Paris (1979).
11. M. S. Daw and M. I. Baskes Phys. Rev. B **12 (29)** (1984) 6443.
12. C. W. B. Grigson and E. Barton, Brit. J. Appl. Phys. **18** (1967) 175.
13. A. Züttel, Ch. Nützenadel, G. Schmid, D. Chartouni, L. Schlapbach, J. Alloys and Compds. **293–295** (1999) 472.
14. J. W. Lee, G. D. Stein, J. Chem. Phys. **91** (1987) 2450.
15. N. M. Jisrawi, A. Pundt, M. Guerdane, H. Teichler, submitted to J. Phys. Chem.
16. R. J. Behm, V. Penka, M. G. Cattania, K. Christmann, G. Ertl, J. Chem. Phys. 78 (1983) 7486.
17. D. Fritsch, G. Bengtson: unpublished results.
18. Pundt A., Kirchheim R., Annual Review Materials Research **36** (2006) 555.